Invited paper

Structural and magnetic properties of Fe/noble metal monatomic multilayers equivalent to L1$_0$ ordered alloys

S. Mitani [a], K. Takanashi [a,d,*], H. Nakajima [b], K. Sato [c], R. Schreiber [d],
P. Grünberg [d], H. Fujimori [a]

[a] IMR, Tohoku University, Sendai 980-77, Japan
[b] Department of Materials Science and Technology, Iwate University, Morioka 020, Japan
[c] Faculty of Technology, Tokyo University of Agriculture and Technology, Koganei, Tokyo 184, Japan
[d] IFF, Forschungszentrum Jülich GmbH, D-52425 Jülich, Germany

Abstract

Alternate monatomic layer deposition by MBE is proposed as a new method to prepare L1$_0$ ordered alloys. A highly-ordered single crystal of Fe–Pt alloy was obtained. Furthermore, the L1$_0$ ordered structure was artificially fabricated for an Fe–Au alloy although it does not exist in the equilibrium phase diagram. The magnetic properties of the ordered Fe–Pt and Fe–Au alloys are described.

1. Introduction

Atomic layer deposition techniques using MBE have been improved for the last decade in order to control well-defined layered structures on an atomic scale; these exhibit novel physical properties, i.e., enhanced magnetoresistance, oscillating exchange coupling, large perpendicular anisotropy, etc. [1]. Such techniques make it possible to fabricate ordered alloys with layered structures artificially. A typical example is the L1$_0$ ordered structure, which consists of alternate stacking of two different atomic planes as shown in Fig. 1. The L1$_0$ ordered structure is generally produced by heat treatment of alloy samples below the order–disorder transformation temperature.

Recently we have been trying the artificial fabrication of a L1$_0$ ordered structure by alternate deposition of Fe and noble metal (Pt or Au) monatomic layers [2,3]. The Fe–Pt system has natural L1$_0$ ordered structure around equiatomic composition in the equilibrium phase diagram [4]. The ordered Fe–Pt alloy is known to show a large magnetocrystalline anisotropy along the c-axis [5], and to be a fascinating material for application as a permanent magnet. On the other hand, the Fe–Au system has a peritectic-type phase diagram and neither intermediate phase nor intermetallic compound exists in the equilibrium phase diagram [4]. The solubility limits of Au to Fe, and of Fe to Au, are both very low at room temperature. How-

ever, the lattice mismatch between bcc Fe and fcc Au is very small ($\sqrt{2} a_{Fe} \approx a_{Au}$), and good epitaxial growth for Fe/Au (100) multilayers was reported by several groups [6–8]. As shown in Fig. 1, this suggests a possibility to fabricate artificially the ordered Fe–Au alloy with the L1$_0$ ordered structure.

This paper describes our recent studies on fabrication, structure and magnetic properties of artificially fabricated ordered Fe–Pt and Fe–Au alloys with the L1$_0$ structure.

2. Experiments

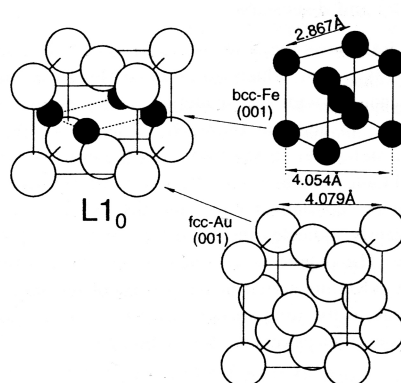The samples were prepared on polished MgO (100) substrates by UHV deposition with two independent e-guns.

Fig. 1. Tetragonal L1$_0$ ordered structure compared with the crystal structures of Fe (bcc) and Au (fcc).

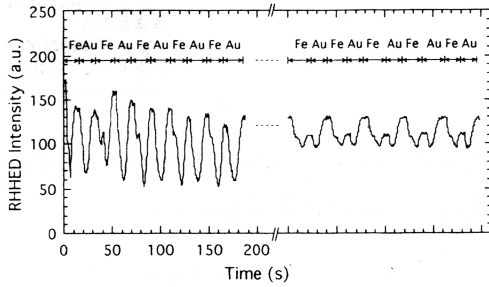* Corresponding author. Fax: +81-22-215-2096; email: koki@magmate.imr.tohoku.ac.jp.

Fig. 2. Oscillation of the RHEED intensity during the growth of the [Fe/Au]$_{100}$ film. The data for the first 10 ML and the last 10 ML are shown.

One monatomic layer (ML) of Fe and 1 ML of Pt (Au) were alternately deposited on the Pt (Au) buffer layer. The substrate temperatures (T_s) for the Fe 1 ML/Pt 1 ML and Fe 1 ML/Au 1 ML growth were 500°C and 70°C, respectively. The repetition of Fe 1 ML and Pt (Au) 1 ML was 100 times. Hereafter, samples prepared by alternate monatomic layer deposition will be designated as [Fe/Pt (or Au)]$_{100}$.

Further details of the preparation procedure were described in previous papers [2,3]. In situ RHEED observation indicated layer-by-layer growth with the orientational relationship of Fe[100]∥Pt (or Au) [110] in the film plane. For the Fe 1 ML/Au 1 ML, particularly, oscillation of the RHEED intensity was observed throughout the 100 layers deposited; a typical example is shown in Fig. 2. However, the monolayer control was made mainly by a quartz thickness monitor because the relationship between the RHEED oscillation and the monolayer growth is not so simple [7,9]. The composition was estimated by in situ Auger spectroscopy and ex situ Rutherford backscattering spectrometry (RBS), which confirmed the equiatomic composition within an error of ±5 at%.

3. Results and discussion

Fig. 3(a) shows the X-ray diffraction (XRD) pattern for the [Fe/Pt]$_{100}$ film, which was obtained by a conventional θ–2θ scanning with the scattering vector normal to the film plane. In addition to the (200) peaks of the MgO substrate and the Pt buffer, (001), (002) and (003) peaks of the Fe–Pt alloy can be seen. The (001) and (003) peaks are regarded as superlattice lines, and the existence of these peaks clearly indicates the formation of the L1$_0$ ordered structure. The degree of chemical order can be evaluated from the XRD integrated intensity ratio of the superlattice (001) peak to the fundamental (002) peak, I_{001}/I_{002}. The long range order parameter S is defined as

$$S = (r_{Fe} - c_{Fe})/(1 - s_{Fe}) = (r_{Pt} - c_{Pt})/(1 - s_{Pt}), \quad (1)$$

where $c_{Fe(Pt)}$ is the atomic fraction of Fe(Pt), $s_{Fe(Pt)}$ the

fraction of Fe(Pt) sites (= 0.5), and $r_{Fe(Pt)}$ the fraction of Fe(Pt) sites occupied by the correct atomic species. S is unity for perfectly ordered alloys, and is zero for chemically disordered alloys. Then, the observed I_{001}/I_{002} is expressed as

$$I_{001}/I_{002} = S^2 (I_{001}/I_{002})^*, \quad (2)$$

where $(I_{001}/I_{002})^*$ is the calculated intensity ratio for the perfectly ordered Fe–Pt alloy [10]. For the [Fe/Pt]$_{100}$ film, S is estimated to be approximately 0.7, which is a considerably large value, indicating that the film is close to the perfectly ordered alloy. Furthermore, it is noted that there are no peaks with other indices, except for (00L) (L = 1,2,3...) in the XRD pattern of Fig. 3(a). This suggests that the film is a single crystal with the c-axis normal to the film plane. Thus, the artificial fabrication of the ordered Fe–Pt alloy by alternate monatomic layer deposition has an advantage that a single crystal with a high degree of chemical order can easily be made, in contrast with the difficulty to prepare a high quality bulk sample by heat treatment because a polytwinned microstructure usually arises [11]. [Fe/Pt]$_{100}$ films were also prepared at various T_s in the range from room temperature (RT) to 500°C. We have found that S decreases with decreasing T_s, and T_s = 500°C is the best choice for the preparation of a high quality sample of the ordered Fe–Pt alloy [2].
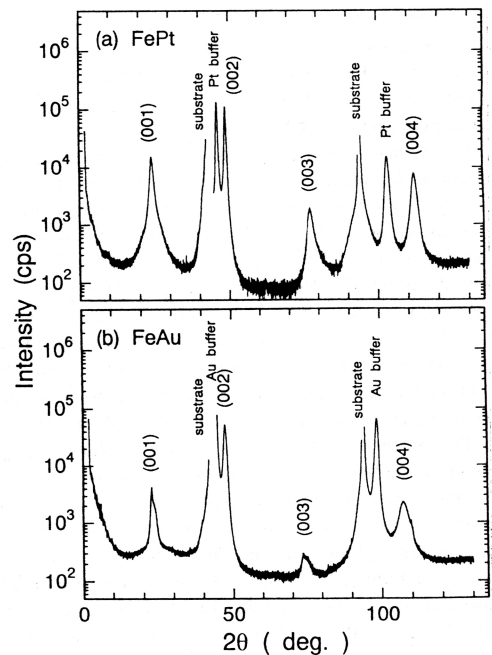

Fig. 3. θ–2θ X-ray diffraction patterns taken with Cu-Kα radiation for (a) the [Fe/Pt]$_{100}$ film and (b) the [Fe/Au]$_{100}$ film.

Fig. 3(b) shows the XRD pattern for the $[Fe/Au]_{100}$ film. The result is similar to that for the $[Fe/Pt]_{100}$ film. In other words, we can see the fundamental (002) peak accompanied with the superstructure (001) and (003) peaks, which confirm the formation of the $L1_0$ ordered structure consisting of alternate stacking of Fe 1 ML and Au 1 ML. S is estimated by the same procedure as that for Fe–Pt, to be approximately 0.3. This value is much smaller than that for Fe–Pt, and it is suggested that the growth condition for Fe 1 ML/Au 1 ML should be still further improved. However, taking into account the fact that the ordered Fe–Au alloy does not exist in the equilibrium state, we may say that $S = 0.3$ is an acceptable value in the first stage of this study. Moreover, we consider that the degree of short range order is higher than that of long range order since the long range order is much more influenced by defects and fluctuation of monatomic layer growth.

The positions of the fundamental (002) peaks give the average (002) spacings, $d_{(002)}$, along the normal direction to the film plane. $d_{(002)}$ for the $[Fe/Au]_{100}$ film is 1.92 Å, which is larger than the simple average of the values for bulk Fe (1.43 Å) and Au (2.04 Å), i.e., $(1.43 + 2.04)/2 = 1.74$ Å, and rather close to that of bulk Au. This situation is very similar to the case of the ordered Fe–Pt alloy stable in nature: $d_{(002)}$ for the ordered Fe–Pt alloy is 1.857 Å, which is larger than the simple average (1.70 Å) of the values for bulk Fe (1.43 Å) and Pt (1.96 Å), and closer to that of bulk Pt.

In order to investigate the tetragonality in the $[Fe/Au]_{100}$ film, XRD was performed by rotating the film in the (110) plane with 2θ fixed at an appropriate angle. Fig. 4 shows the two-dimensional mapping of XRD isointensity contours around the (113) peak in a (110) reciprocal lattice plane. The deviation of the (113) peak position
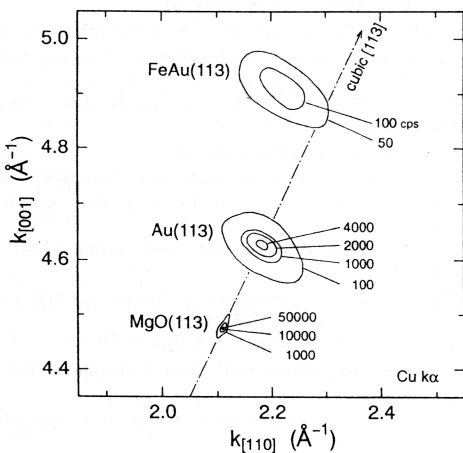

Fig. 4. Two-dimensional mapping of isointensity contours for X-ray diffraction around the (113) peak in a (110) reciprocal lattice plane for the $[Fe/Au]_{100}$ film.

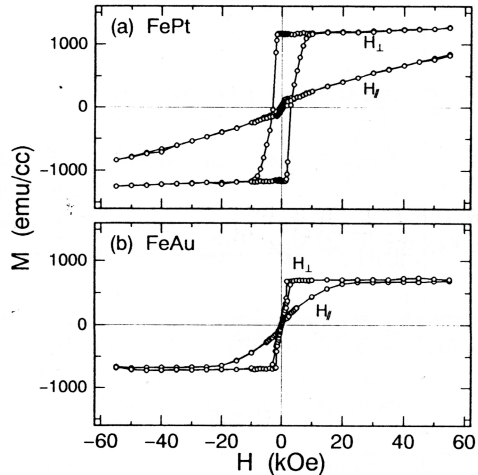
Fig. 5. Magnetization curves at room temperature as a function of applied field parallel ($H_\parallel$) and perpendicular ($H_\perp$) to the film plane of (a) the $[Fe/Pt]_{100}$ film and (b) the $[Fe/Au]_{100}$ film.

from cubic symmetry gives the tetragonality $c/a \approx 0.96$, which is almost the same as that for the ordered Fe–Pt alloy (0.956). Therefore, the $[Fe/Au]_{100}$ film can be regarded as the tetragonal $L1_0$-type ordered Fe–Au alloy with $a = 2d_{(002)} \cdot (a/c) \approx 3.99$ Å and $c = 2d_{(002)} = 3.83$ Å, although chemical order is not perfect.

Fig. 5(a) and (b) show the magnetization curves measured by SQUID at RT as a function of applied field parallel ($H_\parallel$) and perpendicular ($H_\perp$) to the film plane of the $[Fe/Pt]_{100}$ film and of the $[Fe/Au]_{100}$ film, respectively. The $[Fe/Pt]_{100}$ film shows a very large perpendicular magnetic anisotropy comparable to that of the bulk sample [5], and the in-plane magnetization does not saturate even at 5.5 T. The $[Fe/Au]_{100}$ film also shows a considerably large perpendicular magnetic anisotropy, and the uniaxial anisotropy constant K_u is estimated to be 8.5×10^6 emu/cc. The temperature dependence of magnetization for the $[Fe/Au]_{100}$ film was also measured and indicates that the Curie temperature T_C is much higher than RT. The saturation magnetization M_s extrapolated to 0 K is 770 ± 40 emu/cc. Assuming no magnetic moment on Au atoms, the magnetic moment per Fe atom μ_{Fe} is estimated to be $2.5 \pm 0.3 \mu_B$, which is somewhat larger than that of pure Fe ($2.2 \mu_B$). μ_{Fe} exceeding $2.2 \mu_B$ is qualitatively consistent with simple band calculations for Fe/Au multilayers by MacLaren et al. [12]. Regarding the high T_C and the large μ_{Fe} for the $[Fe/Au]_{100}$ film, the reports on the metastable fcc Fe–Au solid solution prepared by vapor quenching [13–15] should be noted.

Fig. 6(a) and (b) show the spectra of polar Kerr rotation θ_K for the $[Fe/Pt]_{100}$ film and for the $[Fe/Au]_{100}$ film, respectively. For comparison, the θ_K spectra for pure Fe and a Fe(22 Å)/Au(48 Å) multilayer film [16] are also
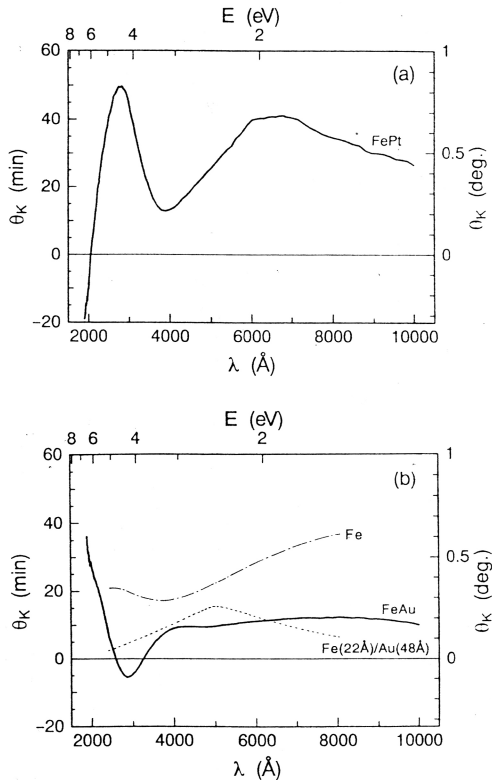
Fig. 6. Spectra of polar Kerr rotation θ_K for (a) the $[Fe/Pt]_{100}$ film and (b) the $[Fe/Au]_{100}$ film, compared with those for pure Fe and a Fe(22 Å)/Au(48 Å) multilayer film.

shown in Fig. 6(a). The $[Fe/Pt]_{100}$ film shows high magneto-optical effect. The θ_K spectrum agrees with that for the co-evaporated Fe–Pt film on MgO at 500°C [10]. The $[Fe/Au]_{100}$ film has fairly large magnitudes of θ_K in the short wavelength range. The spectrum is quite different from those of multilayers which can be explained in terms of the plasma resonance of conduction electrons in Au layers, using the optical constants of pure Fe and Au [16]. We may say that a significant change in the electronic structure of Au atoms occurs in the $[Fe/Au]_{100}$ film. However, there is no complete explanation for the spectrum at present. Exact calculation of the electronic structure taking the relativistic effect into account is necessary.

4. Concluding remarks

$L1_0$-type ordered Fe–Pt and Fe–Au alloys were fabricated artificially by alternate monatomic layer deposition. A highly-ordered single crystal of the ordered Fe–Pt alloy was obtained by this method. The $L1_0$ ordered structure was also obtained for Fe–Au although it does not exist in

the equilibrium phase diagram. The ordered Fe–Au alloy shows large μ_{Fe} exceeding 2.2 μ_B, high T_C compared to RT, large K_u along the c-axis, and fairly large magnitude of θ_K. The high T_C, the large μ_{Fe} and the large θ_K are remarkable features of the artificially ordered Fe–Au alloy, compared with those of ultrathin Fe films sandwiched with thick Au [6]. Furthermore, the large K_u is characteristic of the layered structure of the ordered Fe–Au alloy, in contrast with isotropic Fe–Au alloys prepared by vapor quenching [13–15]. Finally, we remark that since the degree of chemical order is not so large as mentioned earlier, K_u and θ_K in the present work are not unique values for the ordered Fe–Au alloy and they might be further enhanced by improvement of the chemical order, similarly to the case of ordered Fe–Pt alloy [2,10].

References

[1] For a recent review, see J.A.C. Bland and B. Heinrich, Eds., Ultrathin Magnetic Structures (Springer, 1994, Berlin).

[2] S. Mitani, K. Takanashi, M. Sano, H. Fujimori, A. Osawa and H. Nakajima, J. Magn. Magn. Mater. 148 (1995) 163.

[3] K. Takanashi, S. Mitani, M. Sano, H. Fujimori, H. Nakajima and A. Osawa, Appl. Phys. Lett. 67 (1995) 1016.

[4] T.B. Massalski, J.L. Murray, L.H. Bennet and H. Baker, Eds., Binary Alloy Diagrams (American Society of Metals Park, OH, 1986).

[5] O.A. Ivanov, L.V. Solina, V.A. Demshina and L.M. Magat, Fiz. Metal. Metalloved. 35 (1973) 92.

[6] T. Okuyama, Jpn. J. Appl. Phys. 30 (1991) 2053.

[7] Y. Suzuki, H. Kikuchi, M. Taninaka, T. Katayama and S. Yoshida, Appl. Surf. Sci. 60–61 (1992) 820.

[8] A. Fuß, S. Demokritov, P. Grünberg and W. Zinn, J. Magn. Magn. Mater. 103 (1992) L221.

[9] K. Takanashi et al., to be published.

[10] A. Cebollada, D. Weller, J. Sticht, G.R. Harp. R.F.C. Farrow, R.F. Marks, R. Savoy and J.C. Scott, Phys. Rev. B 50 (1994) 3419.

[11] B. Zhang, M. Lelovic and W.A. Soffa, Scripta Metall. 25 (1991) 1577.

[12] J.M. MacLaren, M.E. McHenry, S. Crampin and M.E. Eberhart, J. Appl. Phys. 67 (1990) 5406.

[13] W. Felsch, Z. Angew. Phys. 29 (1970) 217.

[14] G. Marchal, Ph. Mangin and C. Janot, J. Physique Colloq. 36 (1975) C2-91.

[15] T.R. McGuire, J.A. Aboaf and E. Klokholm, J. Appl. Phys. 52 (1981) 2205.

[16] T. Katayama, H. Awano and Y. Nishihara, J. Phys. Soc. Jpn. 55 (1986) 2539.